



STUDY ON SHAKING TABLE TEST OF ± 1100 kV POST INSULATOR MOUNTED ON THE TOP OF THE TRANSFORMER FIREWALL

Sen Lin⁽¹⁾, Yongfeng Cheng⁽²⁾, Zhenlin Liu⁽³⁾, Po Gao⁽⁴⁾, Yuhan Sun⁽⁵⁾

⁽¹⁾ Beijing, China, China Electric Power Research Institute, linsen@epri.sgcc.com.cn

⁽²⁾ Beijing, China, China Electric Power Research Institute, cyf@epri.sgcc.com.cn

⁽³⁾ Beijing, China, China Electric Power Research Institute, liuzhenlin@epri.sgcc.com.cn

⁽⁴⁾ Beijing, China, China Electric Power Research Institute, gaopo@epri.sgcc.com.cn

⁽⁵⁾ Beijing, China, China Electric Power Research Institute, sunyuhan@epri.sgcc.com.cn

Abstract

In electrical substations, some types of porcelain electrical equipment need to be mounted on the top of the transformer firewall. The firewall has a significant seismic response magnification effect on the porcelain electrical equipment. However, lack of investigation on the dynamic magnification effect of firewall raises the earthquake damage risk of the porcelain electrical equipment. ± 1100 kV ultra high voltage (UHV) transmission project represents the highest voltage level, largest transmission capacity and longest transmission distance in the world at present. In order to ensure the seismic safety of electrical equipment on the firewall in ± 1100 kV converter station, the shaking table test of ± 1100 kV post insulator which is mounted on the converter transformer firewall is carried out. The finite element model of the firewall-insulator structure is established. The acceleration time history of earthquake motion on the interface between firewall and post insulator is obtained by the seismic analysis with site artificial wave as input. The peak acceleration on the wall is approximately 5 times higher than the peak ground acceleration. Additionally, the firewall not only increases the acceleration amplitude of ground motion but also changes the spectrum characteristics of ground motion. In the shaking table test of ± 1100 kV insulator, the seismic response laws of the ± 1100 kV insulator excited by site artificial wave and wall wave are obtained. The test results show that the max stress of porcelain insulator induced by 0.2 g site artificial wave is 17.10 MPa and that induced by wall wave increase to 25.93 MPa. In addition, because the firewall changes the seismic spectrum characteristics, the influence of high order modes becomes stronger. As a result, the stress distribution of the porcelain insulator is changed. The dangerous section may not appear at the root of the electrical equipment. The experimental study indicates that dynamic magnification effect of firewall can not be ignored in the design and manufacture process of the electrical equipment installed on the firewall. Besides the flange joint at the root of porcelain electrical equipment, other critical sections should be checked to guarantee that the structural strength meets the seismic requirements.

Keywords: ± 1100 kV post insulator; Firewall; Seismic analysis; Shaking table test



1. Introduction

High voltage power transmission engineering is a crucial part of lifeline project. In the past major earthquakes, the damage of high voltage substation and converter station seriously hindered the power supply in the disaster area. It not only affected the safety and reliability of power grid, but also caused huge social and economic losses [1-3]. In electrical substations, post insulators are installed between conductors with different potentials or between grounding components and conductors, which play the role of mechanical support and electrical insulation simultaneously [4]. Electrical post insulator is important component of electrical substation since failure in such insulator leads to disruption of power supply in many cases. The solid porcelain post is the traditional material of choice for the insulators and has a long history of usage [5], but it is seismically vulnerable. Damage and failure of different equipment post insulators were observed after many earthquakes in the United States, China, New Zealand, Chile, Japan, and Haiti [6]. Most of the insulator damage is attributed to the brittleness of the porcelain posts [7]. Since 1970s, composite post insulators have been gradually adopted [8]. The composite insulator is a relatively new and competitive alternative for porcelain insulator [9-11]. However, the displacement of composite insulator during earthquake is large, which is more likely to cause safety problems in insulation distance.

Mohamed et al. carried out static loading and dynamic shaking table tests on two types of 230 kV disconnect switches post insulators [5]. It is found that composite insulator is much lighter mass than porcelain insulator, which in turn is more favorable from the seismic performance perspective. However, the structural response of composite insulator is comparable to that of porcelain insulator. Siamak et al. studied the static and dynamic mechanical behaviors of electrical hollow composite post insulator through a series of tests, which comprise pull and cyclic quasi-static tests in addition to impact hammer tests [12]. An analytical model is derived from the mechanical behavior to deduce the response of the un-damaged and damaged post insulator. Li et al. investigated the seismic fragility of composite insulator based on the theory of probabilistic seismic fragility analysis [13]. Zhu et al. established the two degree of freedom theoretical model and dynamic equation of interconnected electrical equipment [14]. The seismic response law of ± 800 kV composite post insulators under seismic action was discussed. Additionally, influences of the conductor stiffness and equipment stiffness on the seismic performance of the connected equipment were analyzed by using structural dynamics theoretical analysis method. Xie et al. studied the seismic performance of ± 800 kV composite post insulator and simplified calculation method of seismic response for equipment interconnected by rigid bus [15].

Abundant achievements have been made in past studies on the seismic behavior of post insulator and its interconnection system. However, the lack of information associated to the seismic performance of ± 1100 kV insulator is detrimental to the design of the highest voltage level power transmission and transformation project in the world at present. Moreover, the previous research mainly focused on the post insulator which is installed on the ground or steel support. The magnification factor of the support on the seismic response of the electrical equipment has already been stipulated in the relevant code for seismic design [16,17]. However, very meager efforts have been dedicated to researching the seismic response of the post insulator which is applied on the firewall. The previous research indicates that the potential seismic risk for electrical equipment on the firewall is serious due to the dynamic magnification effect of firewall is significant [18].

A finite element model of the converter firewall and the post insulator on it in ± 1100 kV converter station is established. The site artificial wave is used as input to accomplish the seismic analysis. The acceleration time history of earthquake motion on the interface between firewall and post insulator is obtained. The shaking table test of ± 1100 kV post insulator is carried out. The seismic performance of ± 1100 kV insulator is investigated. The seismic response law of ± 1100 kV insulator excited by site artificial wave and wall wave is studied. The influence of firewall on the seismic response of post insulator mounted on the firewall is analyzed. It contributes to seismic evaluation and design of ± 1100 kV post insulator and electrical equipment which installed on the fire wall of UHV station.



2. Seismic analysis of ± 1100 kV post insulator - firewall structure

The porcelain post insulator mounted on the firewall in Guquan ± 1100 kV converter station is selected to conduct this study. The total height of the post insulator is 12 m. The total weight of the post insulator is 3.45 ton. The whole post insulator is composed of 6 pieces of porcelain post connected by steel flange joints. The height of each porcelain post is 2 m. The diameter of each porcelain post (excluding the umbrella skirt) is between 280 mm – 320 mm. The elastic modulus of the porcelain post is 112 GPa. The failure stress of the porcelain post insulator provided by the manufacturer is 60 MPa.

Because the service location of the ± 1100 kV post insulator is on the top of firewall, the variation of earthquake motion from ground to the top of firewall should be considered. The current Chinese standard provides the dynamic magnification factor of the steel support for the UHV equipment [19]. For electrical equipment and devices installed on the second and third floors indoors, the dynamic magnification factor of buildings shall be taken as 2.0 [16]. However, standards and researches related to the dynamic magnification effect of the firewall on the electrical equipment are extremely scarce.

As shown in Fig. 1, the numerical model of ± 1100 kV post insulator – firewall structure is developed. The installation height of the post insulator is 9.5 m. The thickness of the wall is 0.4 m. The length of the wall is 24 m. The direction perpendicular to firewall surface is defined as Y direction in this paper. The vertical direction is defined as Z direction. Thus X direction can be determined, which is parallel to the firewall surface. The acceleration time history at the bottom of the post insulator can be simulated by inputting the site artificial wave of Guquan ± 1100 kV converter station. In addition, it is adopted as input signal for the shaking table test conducted in this study, which is referred to as wall wave in the following content.

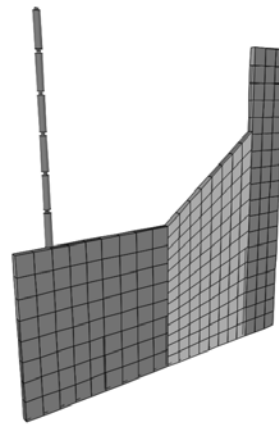


Fig. 1 – Finite element model of firewall - post insulator structure

The earthquake influence coefficient curve of the earthquake action can be calculated in accordance with relevant standard [17], as shown in Fig. 2.

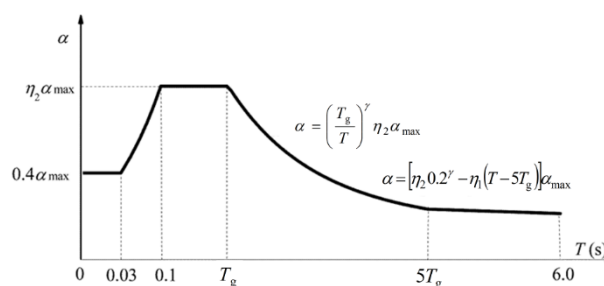


Fig. 2 – Seismic acceleration response spectrum for UHV converter station



The design acceleration of ground motion for electrical installation in Guquan ± 1100 kV converter station is 0.15 g. The design characteristic period of ground motion is 0.6 s. According to the seismic ground motion parameters, the expression of the earthquake influence coefficient curve shall be determined by Eq. (1) - Eq. (4). Additionally, the corresponding acceleration time history curve can be generated from it. According to relevant standard [17], the maximum vertical peak ground acceleration shall be taken as 80% of the maximum horizontal ground acceleration. The acceleration time history curve of horizontal direction ground motion for Guquan is shown in Fig. 3, which is referred to as site artificial wave in the following subsections.

$$\alpha = \begin{cases} 0.4\alpha_{\max} & 0 \leq T < 0.03 \\ \left[0.4 + \frac{\eta_2 - 0.4}{0.07}(T - 0.03) \right] \alpha_{\max} & 0.03 \leq T < 0.1 \\ \eta_2 \alpha_{\max} & 0.1 \leq T < T_g \\ \left(\frac{T_g}{T} \right)^\gamma \eta_2 \alpha_{\max} & T_g \leq T < 5T_g \\ \left[\eta_2 0.2^\gamma - \eta_1 (T - 5T_g) \right] \alpha_{\max} & 5T_g \leq T < 6.0 \end{cases} \quad (1)$$

$$\gamma = 0.9 + \frac{0.05 - \xi}{0.3 + 6\xi} \quad (2)$$

$$\eta_1 = 0.02 + \frac{0.05 - \xi}{4 + 32\xi} \quad (3)$$

$$\eta_2 = 1 + \frac{0.05 - \xi}{0.08 + 1.6\xi} \quad (4)$$

where α is the earthquake influence coefficient, α_{\max} is the maximum value of earthquake influence coefficient, T is the natural vibration period of structure, γ is the attenuation index, η_1 is the adjustment coefficient of the linear declining segment, η_2 is the adjustment coefficient of damping, ξ is the damping ratio of structure.

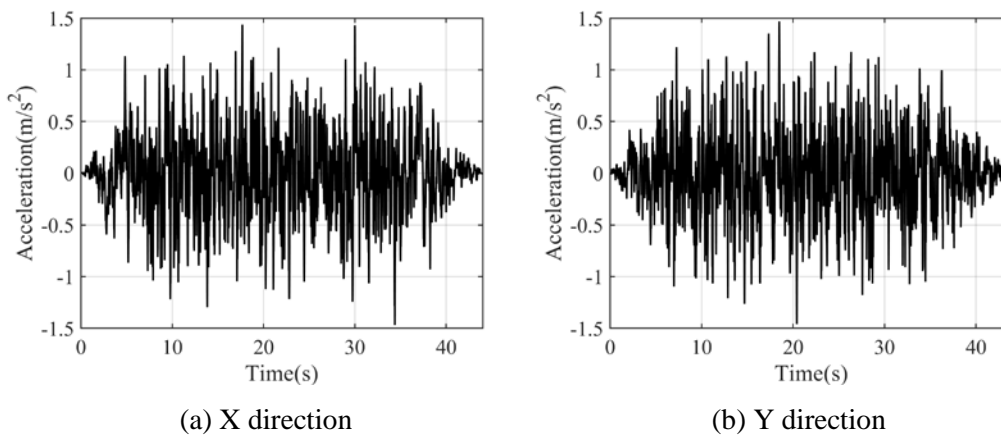


Fig. 3 – Acceleration time history of Guquan ground

Fig. 4 shows the acceleration time history at the bottom of the post insulator obtained by the numerical simulation. It is evident that the difference between the site artificial wave and the wall wave in X direction is slight. However, the peak acceleration of the wall wave in Y direction is approximately 5 times that of the



site artificial wave, indicating that the Y direction is the seismic unfavorable direction. The firewall has obvious dynamic magnification effect on seismic action in this direction.

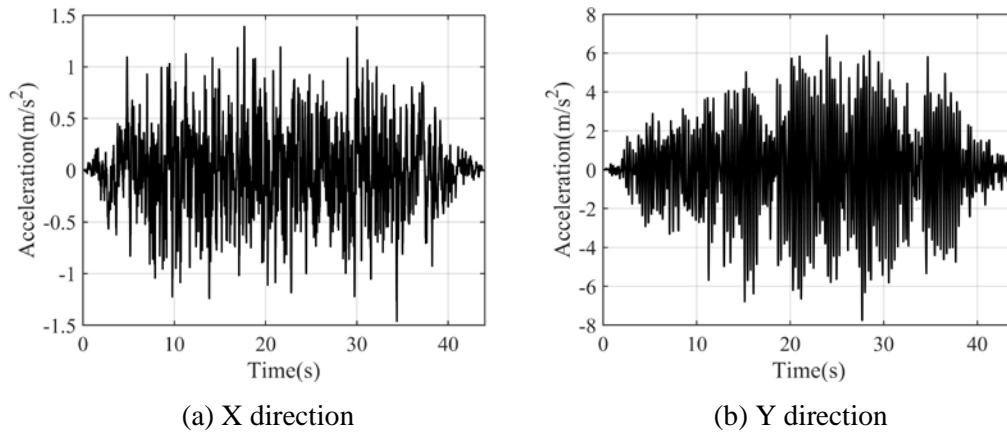


Fig. 4 – Acceleration time history at the bottom of $\pm 1100\text{kV}$ post insulator

Fig. 5 (a) and (b) are the comparisons of response spectrum of the site artificial wave and the wall wave in X and Y directions respectively. It is clearly seen that the spectrum characteristics of the site artificial wave and wall wave in X direction are basically uniform. In Y direction, the maximum value of acceleration response spectrum at the top of the wall appears near the fundamental natural frequency of the firewall. In the range of flat segment and declining segment, the response spectrum value of wall wave is much higher than that of site artificial wave. It shows that the firewall has strong dynamic magnification effect on the seismic response of the electrical equipment installed on the firewall in Y direction from the aspect of frequency domain.

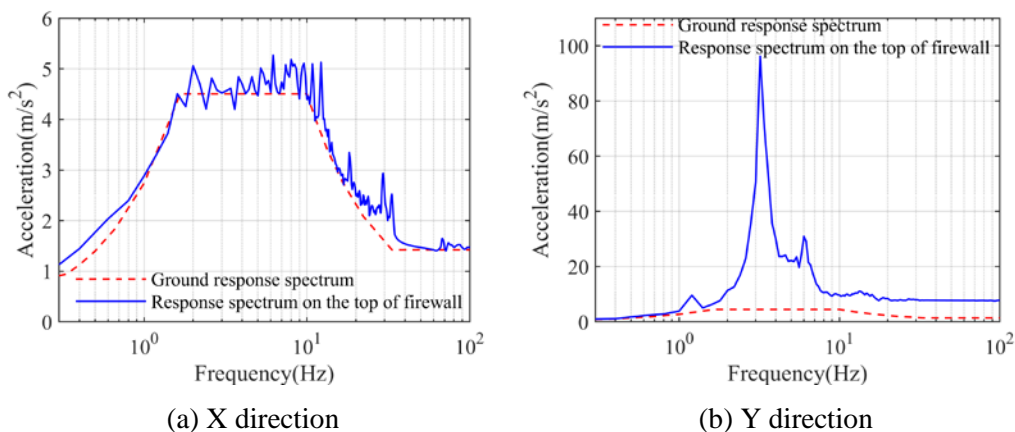


Fig. 5 – Comparison of response spectrum between site artificial wave and wall wave

3. Shaking table test of $\pm 1100\text{kV}$ post insulator

The seismic performance of full-scale $\pm 1100\text{ kV}$ post insulator is investigated through seismic simulation shaking table test. Displacement sensors are arranged on the top of the post insulator and shaking table. Accelerometers are arranged on the top of each porcelain post and shaking table. Four strain gauges in X+, X-, Y+, Y- directions are arranged symmetrically at the root of each porcelain post. Fig. 6 shows the arrangement of monitoring points.

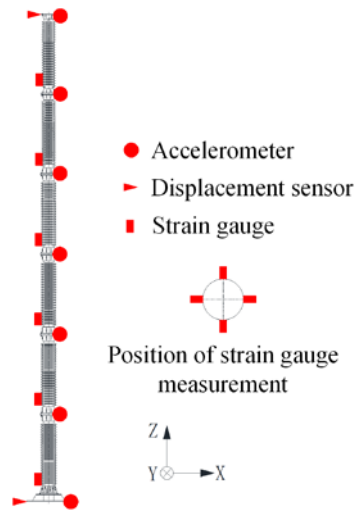


Fig. 6 – Layout of sensor arrangement

The test conditions are shown in Table 1. Owing to the axisymmetric structure, single horizontal seismic excitation can be adopted in the shaking table test [20]. The site artificial wave and wall wave are adopted as input signals for the experiment. Four ranks of earthquake acceleration are considered in the test, namely 0.05 g, 0.1 g, 0.15 g and 0.2 g. The acceleration level of site artificial wave is equal to its target peak acceleration. That of wall wave can be considered as peak ground acceleration of site artificial wave in the above-mentioned finite element simulation.

Table 1 – Shaking table test conditions

Test number	Test condition	Direction	Acceleration level (g)	Test number	Test condition	Direction	Acceleration level (g)
1	white noise	XYZ	0.05	12	wall wave	X	0.05
2	site artificial wave	X	0.05	13	wall wave	X	0.10
3	site artificial wave	X	0.10	14	wall wave	X	0.15
4	site artificial wave	X	0.15	15	wall wave	X	0.20
5	site artificial wave	X	0.20	16	white noise	XYZ	0.05
6	white noise	XYZ	0.05	17	wall wave	Y	0.05
7	site artificial wave	Y	0.05	18	wall wave	Y	0.10
8	site artificial wave	Y	0.10	19	wall wave	Y	0.15
9	site artificial wave	Y	0.15	20	wall wave	Y	0.20
10	site artificial wave	Y	0.20	21	white noise	XYZ	0.05
11	white noise	XYZ	0.05	-	-	-	-

Fig. 7 shows the general overview of the specimen in the shaking table test.



Fig. 7 – General overview of the post insulator

4. Test results and discussion

4.1 Natural vibration characteristics

To acquire the dynamic characteristics of ± 1100 kV post insulator, the frequency response function of the specimen is obtained through the test condition of white noise inserted before and after the seismic test condition. The natural frequency of the specimen can be determined from that. Furthermore, deterioration and damage of the specimen can be identified from the variation in natural frequency. Several free vibration periods are selected from the declining segment of acceleration time history at the top of the specimen. Additionally, the damping ratio of the specimen can be derived from the peak accelerations of the first and last periods.

Table 2 shows the results of dynamic characteristics of ± 1100 kV post insulator before and after shaking table test. The deviations of frequencies between X direction and Y direction are less than 7%. The natural frequency of the specimen after the seismic test is consistent with that before the seismic test basically. Through the analysis of every white noise condition in the test, it is found that frequency response functions match well with each other, which shows that the dynamic characteristics of the test piece keep uniform in the test. The damping analysis results listed in Table 2 show that the damping ratio of the specimen varies from 1.42% ~ 2.04%.

Table 2 – Dynamic characteristics of ± 1100 kV post insulator

Test number	Frequency in X direction (Hz)		Damping ratio (%)	Frequency in Y direction (Hz)		Damping ratio (%)
	First mode	Second mode		First mode	Second mode	
1	1.47	8.12	1.56	1.41	7.58	1.42
21	1.44	8.00	2.04	1.39	7.47	1.47

The finite element modal analysis shows that the first-order frequency is 1.44, and the second-order frequency is 8.36. The reasonably close match between the experimental and simulated results reveals the validity of the proposed finite element model.



4.2 Stress of the post insulator and validation of finite element model

Fig. 8 shows the maximum stress at the root of each porcelain post for every test condition. It reflects the stress distribution of the specimen. It can be seen that maximum stress of the upper three porcelain posts increases linearly with the decreasing height. However, the stress distribution of the three porcelain posts at the bottom has non-linear characteristics with height variation obviously. The reason is that the upper three porcelain posts are the same, but the three porcelain posts at the bottom adopt the differential design, which makes the post diameter increases from the 4th post to the 6th post. The growth trend of stress becomes slow from the 4th post on account of the section diameter increment. The maximum stress of the 4th post even less than that of the 3th post in some test conditions.

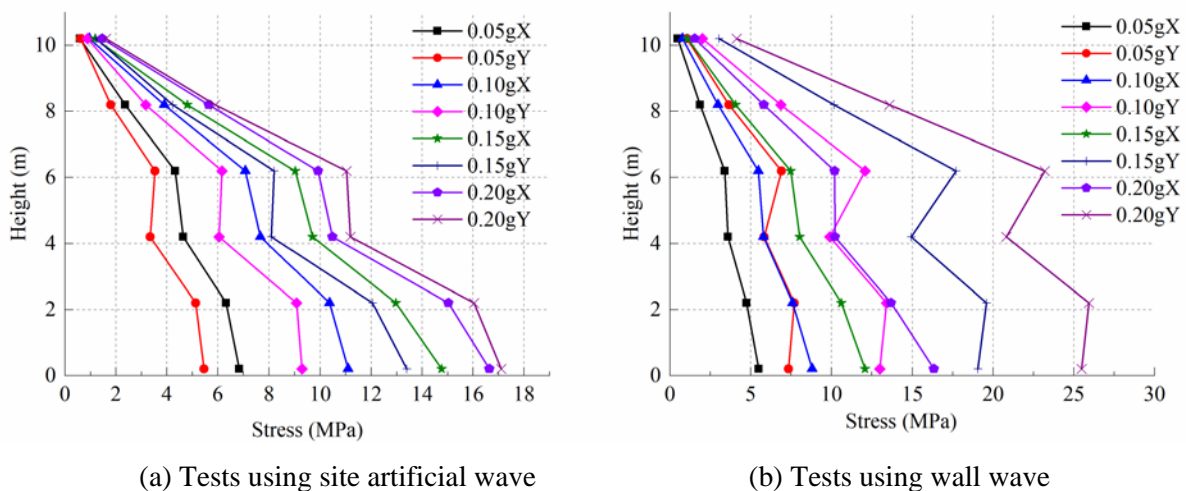
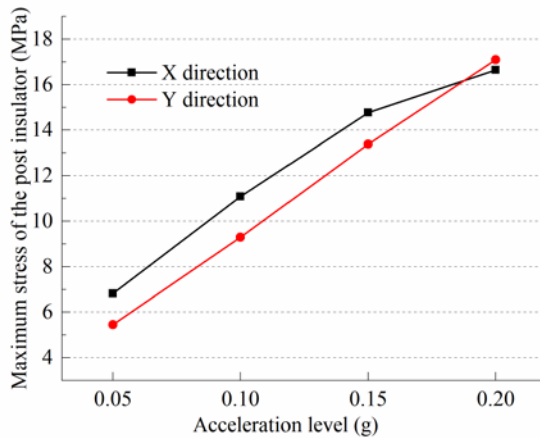


Fig. 8 – Maximum stress at the root of each porcelain post of ± 1100 kV post insulator

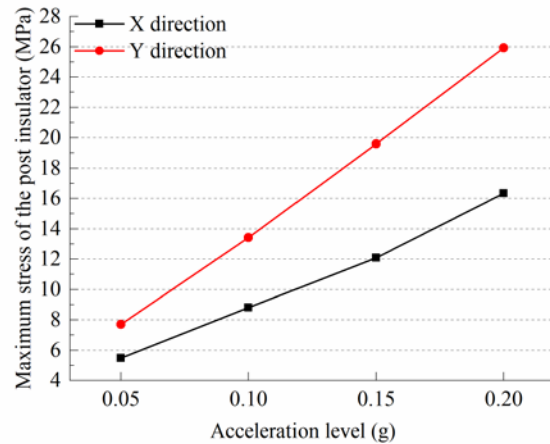
During the test with input of site artificial wave, the difference between the maximum stress of each post in X direction and that in Y direction is not remarkable. The maximum stress of the whole specimen appears at the root of the post insulator. During the test with input of wall wave in X direction, the stress distribution is similar to that during the test with input of site artificial wave in X direction because the wall wave resembles the site artificial wave in X direction. The stress distribution during the test with input of wall wave in Y direction implies that more high order modes participate the vibration of the post insulator. The maximum stress in test 10 appears at the root of the post insulator, which is 17.10 MPa. In test 20, the maximum stress appears at the root of penultimate post instead of the 6th post, which is 25.93 MPa. This is also the maximum stress of the dangerous section in all test conditions. Considering that the failure stress of high-strength porcelain is 60 MPa, the minimum stress safety factor of the specimen among all test conditions is 2.31, which can meet the seismic requirement of Guquan ± 1100 kV converter station.

Fig. 9 compares the maximum stress results of the whole post insulator for different acceleration levels. For 0.05 g to 0.2 g acceleration level, the maximum stress of the whole specimen increases with the increasing peak ground acceleration. During the test with input of wall wave, the growth rate of the stress in Y direction is greater than that in X direction.

Table 3 compares the maximum stress of each porcelain post forecasted by the finite element method and the experimental results for test 20. The reasonably close match between the test and simulated results indicates that the developed finite element model is effective. The deviation of maximum stress between simulated and experimental result is controlled within 16% for each porcelain post. Especially the maximum stress error of the three posts at the bottom is less than 6%, which shows that accuracy of the finite element simulation can meet the engineering design requirements.



(a) Tests using Site wave



(b) Tests using Wall wave

Fig. 9 – Comparison of maximum stress results of ± 1100 kV post insulator

Table 3 – Comparison of testing stress and simulated stress

Post	1 st	2 nd	3 rd	4 th	5 th	6 th
Test result (MPa)	4.13	13.59	23.19	20.81	25.93	25.48
Calculated result (Mpa)	3.99	12.51	19.64	21.48	24.70	24.15
Error (%)	3.39	7.95	15.31	3.22	4.74	5.22

4.3 Displacement of the post insulator

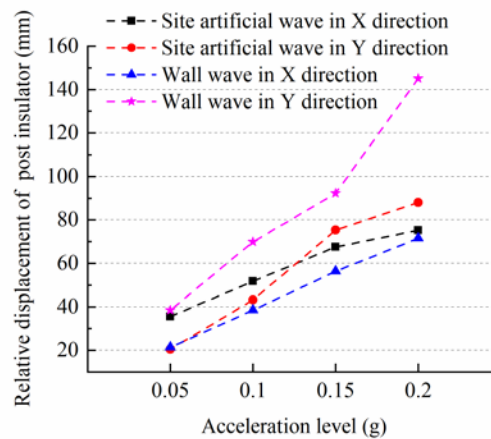
Fig. 10– Maximum relative displacement results of ± 1100 kV post insulator

Figure 10 illustrates the maximum relative displacements of ± 1100 kV post insulator for different test conditions. The relative displacement is determined as the absolute value of the difference between the top displacement of the post insulator and the table displacement during the seismic event. The maximum relative displacement of the specimen in test 20 is 145.16 mm. The maximum displacement of the post insulator increases with the increasing acceleration level. Based on the relative displacement result during the test with input of site artificial wave in Y direction, it's not difficult to conclude that the firewall has great magnification effect on the dynamic response of the electrical equipment mounted on it from the aspect of displacement.



5. Conclusion

To investigate the seismic performance of the post insulator installed on the converter firewall in ± 1100 kV converter station, the finite element model of the firewall - post insulator structure is developed. The acceleration time history on the interface between firewall and post insulator and the seismic response of ± 1100 kV post insulator are obtained. The shaking table test using the artificial site wave and wall wave as input is carried out. Following conclusions are obtained.

(1) The firewall has significant dynamic magnification effect on earthquake in the direction which is perpendicular to firewall surface. When the earthquake motion is transmitted to the top of the wall, the acceleration amplitude increases dramatically, approximately 5 times than that of the ground motion. Furthermore, the spectrum characteristics of the ground motion change significantly. In the direction which is perpendicular to firewall surface, the maximum value of acceleration response spectrum at the top of the wall occurs near the fundamental natural frequency of the firewall. In the range of flat segment and declining segment, the response spectrum value of wall wave is much higher than that of site artificial wave.

(2) Due to the change of seismic spectrum characteristics induced by firewall, more high order modes participate the vibration of the post insulator mounted on the firewall. The dangerous section may no longer appear at the root of the post insulator as usual. The maximum stress may occur at the penultimate post or middle position of the post insulator. Therefore, besides considering structural design of root connection, attention should be paid to the strength of the penultimate post and the middle part for the electrical equipment installed on the firewall.

(3) The dynamic response of the post insulator has been significantly amplified because of the firewall. The maximum stress of ± 1100 kV post insulator is 17.10 MPa during the test with artificial site wave of 0.2 g acceleration level, while that reaches 25.93 MPa during the test with wall wave of 0.2 g acceleration level. the minimum stress safety factor of the specimen among all test conditions is 2.31, which can meet the seismic requirement of Guquan ± 1100 kV converter station.

(4) For the ± 1100 kV post insulator in the test, maximum stress of the upper three porcelain posts increases linearly with the decreasing height. However, the stress distribution of the three porcelain posts at the bottom has non-linear characteristics with height variation. The reason is that the upper three porcelain posts are the same, but the three porcelain posts at the bottom adopt the differential design, which makes the post diameter increases from the 4th post to the 6th post.

6. References

- [1] Qiu N, Cheng Y, Zhong M, Lu Z, Zhu Z, Lu X (2015): Progress and prospect in seismic research of 1000 kV UHV AC electrical equipment. *High Voltage Engineering*, **41** (5), 1732-1739.
- [2] Seyed AZ, Mahmood H, Mohsen GA (2016): Seismic failure probability of a 400 kV power transformer using analytical fragility curves. *Engineering Failure Analysis*, **70**, 273-289.
- [3] Li S, Tsang HH, Cheng Y, Lu Z (2017): Considering seismic interaction effects in designing steel supporting structure for surge arrester. *Journal of Constructional Steel Research*, **132**, 151-163.
- [4] Editorial Committee of China Electric Power Encyclopedia (2014): *China Electric Power Encyclopedia*. Chia Electric Power Press.
- [5] Mohamed AM, Khalid MM (2016): Structural performance of porcelain and polymer post insulators in high voltage electrical switches. ASCE, *Journal of Performance of Constructed Facilities*, 2016, 04016002, 1-11.
- [6] Fujisaki E, Takhirov S, Xie Q, Mosalam KM. (2014): Seismic vulnerability of power supply: Lessons learned from recent earthquakes and future horizons of research. *9th International Conference on Structural Dynamics EURO-DYN*, Porto, Portugal.



- [7] Seyed AZ, Mahmood H, Mohsen GA (2017): Evaluation of power substation equipment seismic vulnerability by multivariate fragility analysis: A case study on a 420 kV circuit breaker. *Soil Dynamics and Earthquake Engineering*, **92**, 79-94.
- [8] Papailiou KO, Schmuck F (2013): *Reinforced Concrete Slabs*. Springer-Verlag Berlin Heidelberg.
- [9] Wang L, Wang C, FU G, Shan Z (2011): Antiseismic characteristics of composite post insulator for smoothing reactors on UHVDC. *High Voltage Engineering*, **37** (9), 2081-2088.
- [10] Sun Y, Cheng Y, LU Z, Lin S, Wang X, Qiao Z (2017): Study on earthquake simulation shaking table test of 1100 kV composite external insulation bushing. *High Voltage Engineering*, **43** (10), 3224-3230.
- [11] Sun Y, Cheng Y, Wang X, LU Z, Qiu N, Lin S, Zhang Q (2018): Studies on earthquake simulation shaking table tests of 1100kV gas insulated switchgear composite external insulation bushings. *Proceedings of the CSEE*, **38** (7), 2179-2187.
- [12] Siamak E, Kiarash MD, Nicholas DO, Andrei MR (2015): Mechanical behavior of electrical hollow composite post insulators: Experimental and analytical study. *Engineering Structures*, **93**, 129-141.
- [13] Li S, Lu Z, Zhu Z, Liu Z, Cheng Y, Lu X (2016): Dynamic properties and seismic fragility of substation composite insulators. *Engineering Mechanics*, **33** (4), 91-97.
- [14] Zhu Z, Zhang L, Cheng Y, Lu Z, Liu Z, Li S, Zhong M (2018): Seismic response analysis on connected circuit of the composite insulator of ± 800 kV converter station. *Advanced Engineering Sciences*. **50** (6), 23-30.
- [15] Xie Q, Zhang Y, He C, Yang Z (2019): Experimental and analytical study on seismic performance of ± 800 kV UHVDC composite post insulator interconnected by rigid bus. *High Voltage Engineering* (Accepted).
- [16] MOHURD (2013): Code for seismic design of electrical installations. GB 50260-2013, China Planning Press, Beijing.
- [17] SGCC (2018): Technical code for seismic technology of ultra-high voltage direct-current equipment. Q/GDW 11677-2017, Beijing.
- [18] Lin S, Cheng Y, Lu Z, Meng X, Guo X, Fu Y (2017): Investigation on seismic performance and shock absorption of arrester in ± 1100 kV converter station. *High Voltage Engineering*. **43** (10): 3198-3207.
- [19] CSEE (2017): Code for seismic design of 1000 kV substations. T/CSEE 0010-2016, Chia Electric Power Press, Beijing.
- [20] Lin S, Cheng Y, Meng X, Sun Y, Lu Z, Zhang Q (2019): A study on seismic performance optimization of 1000 kV capacitor voltage transformer. *Journal of Vibration and Shock*. **24**: 1-10.